Article

Dendritic Molecular Switch: Chiral Folding and Helicity Inversion

Xuan Jiang, Young-Kwan Lim, Bong June Zhang,
Elizabeth A. Opsitnick, Mu-Hyun Baik, and Dongwhan Lee

J. Am. Chem. Soc., **2008**, 130 (49), 16812-16822 • DOI: 10.1021/ja806723e • Publication Date (Web): 11 November 2008

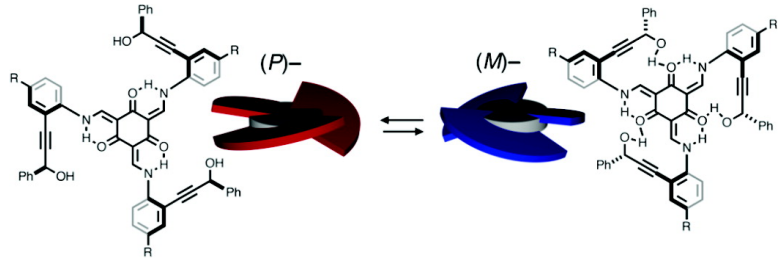

More About This Article

Additional resources and features associated with this article are available within the HTML version:

- Supporting Information
- Access to high resolution figures
- Links to articles and content related to this article
- Copyright permission to reproduce figures and/or text from this article

View the Full Text HTML

J|A|C|S
ARTICLES

Published on Web 11/11/2008

Dendritic Molecular Switch: Chiral Folding and Helicity Inversion

Xuan Jiang, Young-Kwan Lim, Bong June Zhang, Elizabeth A. Opsitnick, Mu-Hyun Baik, and Dongwhan Lee*

Department of Chemistry, Indiana University, 800 East Kirkwood Avenue, Bloomington, Indiana 47405

Received August 25, 2008; E-mail: dongwhan@indiana.edu

Abstract: Appropriately designed chemical architectures can fold to adopt well-defined secondary structures without the need for structural motifs of biological origin. We have designed tris(*N*-salicylideneaniline)-based hyperbranched molecules that spontaneously collapse to compact three-blade propeller geometry of either (*P*)- or (*M*)-handedness. For a homologous series of compounds, a direct correlation was established between the absolute screw sense, either (*P*)- or (*M*)-, of this helical folding and the absolute configuration, either (*R*)- or (*S*)-, of the chiral alcohol groups introducing local asymmetric bias to the conformationally restricted molecular backbone. ^{1}H NMR and CD spectroscopic studies provided significant insights into structural folding and unfolding of these chiral molecules in solution, which proceed via reversible assembly and disassembly of the C_3-symmetric hydrogen-bonding network. Notably, solvents profoundly influenced this dynamic process. A strong correlation between the solvent donor number (DN) or solvent basicity (SB) parameters and the change in the Cotton effects pointed toward specific O−H···solvent interactions that drive structural unfolding and eventual refolding to apparently opposite helicity. This unusual chirality inversion process could also be induced by installation of chemical protecting groups that simulate specific solvent−solute interactions. Removal of this covalent mimic of the solvent shell restored the original screw sense of the parent molecule, thus establishing the feasibility of covalently triggered helicity inversion as a new mode of operation for chiroptical molecular switches.

Introduction

Controlling the conformational bias of inherently flexible chemical structures is a formidable challenge. Spontaneous folding of biological macromolecules, however, proceeds with an extraordinary degree of control over the spiral arrangement of their linear sequences, as exemplified by the well-defined secondary structures of α-helical polypeptides or polynucleotides.[1] Exactly how the weak noncovalent interactions among local carbon-centered chirality collectively translate to global helicity of preferred handedness still remains to be elucidated. During past decades, this important question of cooperativity[2] has stimulated the design, synthesis, and application of helically folding molecular and supramolecular structures.[3,4]

As was demonstrated by others, a delicate interplay of noncovalent interactions promotes well-defined conformations of linear foldamers.[5] This conceptual framework should readily be extended to dendritic structures, in which the making and breaking of symmetrically positioned weak bonds can drive addressable conformational switching.

Unidirectional tilting of three bulky aryl groups around a C_3-symmetric core can furnish with equal probability either a right-handed (*P*)- or left-handed (*M*)-isomer of a three-bladed propeller geometry (Scheme 1).[6−8] Introduction of appropriate chiral auxiliaries as part of R, however, can potentially bias this dynamic process to increase the population of one helix-sense over the other (Scheme 1).

(1) van Holde, K. E.; Johnson, W. C.; Ho, P. S. *Principles of Physical Biochemistry*; 2nd ed.; Pearson Prentice Hall: Upper Saddle River, NJ, 2006.
(2) Williamson, J. R. *Nat. Chem. Biol.* **2008**, *4*, 458–465.
(3) Crego-Calama, M.; Reinhoudt, D. N., Eds. *Supramolecular Chirality*; Springer: Berlin, Germany, 2006.
(4) Hembury, G. A.; Borovkov, V. V.; Inoue, Y. *Chem. Rev.* **2008**, *108*, 1–73.
(5) (a) Gellman, S. H. *Acc. Chem. Res.* **1998**, *31*, 173–180. (b) Hill, D. J.; Mio, M. J.; Prince, R. B.; Hughes, T. S.; Moore, J. S. *Chem. Rev.* **2001**, *101*, 3893–4011. (c) Cubberley, M. S.; Iverson, B. L. *Curr. Opin. Chem. Biol.* **2001**, *5*, 650–653. (d) Cheng, R. P.; Gellman, S. H.; DeGrado, W. F. *Chem. Rev.* **2001**, *101*, 3219–3232. (e) Gong, B. *Chem. Eur. J.* **2001**, *7*, 4336–4342. (f) Schmuck, C. *Angew. Chem., Int. Ed.* **2003**, *42*, 2448–2452. (g) Huc, I. *Eur. J. Org. Chem.* **2004**, 17–29. (h) Stone, M. T.; Heemstra, J. M.; Moore, J. S. *Acc. Chem. Res.* **2006**, *39*, 11–20. (i) Li, Z.-T.; Hou, J.-L.; Li, C.; Yi, H.-P *Chem. Asian J.* **2006**, *1*, 766–778. (j) *Foldamers*; Hecht, S.; Huc, I., Eds.; Wiley-VCH: Weinheim, 2007.
(6) For correlated motions in *n*-fold molecular rotors, see:(a) Brydges, S.; Harrington, L. E.; McGlinchey, M. J. *Coord. Chem. Rev.* **2002**, *233−234*, 75–105. (b) Kottas, G. S.; Clarke, L. I.; Horinek, D.; Michl, J. *Chem. Rev.* **2005**, *105*, 1281–1376.
(7) For a general overview of C_3-symmetric chiral systems, see: (a) Moberg, C. *Angew. Chem., Int. Ed.* **1998**, *37*, 248–268. (b) Moberg, C. *Angew. Chem., Int. Ed.* **2006**, *45*, 4721–4723. (c) Gibson, S. E.; Castaldi, M. P. *Angew. Chem., Int. Ed.* **2006**, *45*, 4718–4720.
(8) For conceptually related trinuclear coordination complexes undergoing interconversion between the (*P*)- and (*M*)-isomers through concerted tilting motions of bulky ligands or intramolecular ligand exchange, see:(a) Ikeda, A.; Udzu, H.; Zhong, Z.; Shinkai, S.; Sakamoto, S.; Yamaguchi, K. *J. Am. Chem. Soc.* **2001**, *123*, 3872–3877. (b) Hiraoka, S.; Harano, K.; Tanaka, T.; Shiro, M.; Shionoya, M. *Angew. Chem., Int. Ed.* **2003**, *42*, 5182–5185. (c) Hiraoka, S.; Hirata, K.; Shionoya, M. *Angew. Chem., Int. Ed.* **2004**, *43*, 3814–3818. (d) Hiraoka, S.; Shiro, M.; Shionoya, M. *J. Am. Chem. Soc.* **2004**, *126*, 1214–1218.

10.1021/ja806723e CCC: $40.75

Scheme 1. Unidirectional Tilting of Three Bulky Aryl Groups Furnishes C_3-Symmetric Structures of Either (*P*)- or (*M*)-Helicity[a]

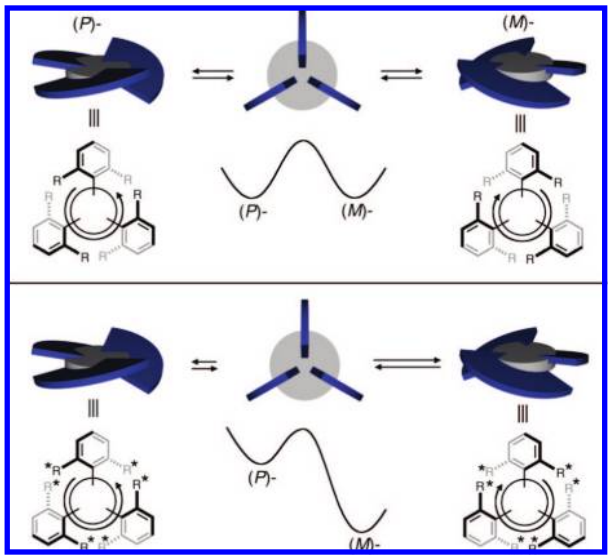

[a] With achiral R groups (top), there is no bias toward either enantiomeric conformer. Intimate contact between chiral R* groups (bottom), however, can induce preferential structural folding to one diastereomer over the other. (*M*)-helix is arbitrarily chosen for the schematic diagram shown at the bottom.

We have recently shown that a three-fold symmetric branched platform represented by tris(*N*-salicylideneamine)s[9−11] can readily be functionalized with hydroxy-terminated aryl-groups.[11d−g] Multiple O−H···O hydrogen bonds connecting adjacent "wing-tip" groups of such molecules function as a conformational lock and enforce overall helical arrangements of the bulky aryls as shown in Scheme 1.[12] We envisioned that this cooperative folding process[3−5,13] could potentially be driven in asymmetric fashion by strategic placement of chiral groups at aryl···aryl contacts. In addition, the C_3-symmetrically disposed hydrogen-bonding network in such constructs can function as a chirality transfer channel, the reversible formation and disruption of which might provide a means to control the global helicity of the molecule.

In this paper, we describe the design of a homologous series of tris(*N*-salicylideneamine)-based chiral dendritic molecules, solution dynamics of their structural folding and unfolding, and a highly unusual interconversion between conformations of apparently opposite helicity. Notably, this new chiral switch[14] can be operated either by interaction with solvent molecules or by manipulation of scissile capping groups.

Results and Discussion

Design Principles for Chiral Induction. Crystallographically characterized compound **1** (Figure 1)[11d] served as a useful design template in our exploratory studies to develop chiral induction models. In the solid state, **1** exists as a 1:1 mixture of right-handed (*P*)- and left-handed (*M*)-conformers, in which a cyclic array of three $O_{hydroxy}-H\cdots O_{hydroxy}-H\cdots O_{keto}$ hydrogen bonds assists unidirectional tilting of three bulky aryls propagating from the C_3-symmetric tris(*N*-salicylideneamine) core. We noted that the methyl substituents on the six tertiary alcohol groups of **1** are brought into distinctively different steric environments upon structural folding, with three CH_3 groups (in dotted circles) pointing *toward* and the other three (in solid circles) pointing *away* from the molecular core (Figure 1). As such, structural modification at these positions to introduce chiral alcohol groups was expected to induce sufficient steric bias to energetically differentiate the diastereomeric (*P*)- and (*M*)-helixes.

This intuitive chirality transfer model was evaluated quantitatively using density functional theory (DFT) calculations on the model compound **2**, which was constructed by replacing the six "wing-tip" $-C(CH_3)_2OH$ groups of **1** with $-C^*H(C_6H_5)OH$ fragments. The two substituents, i.e., H and C_6H_5, on these chiral alcohol groups were intentionally chosen in order to maximize the steric differentiation and thus the relative stability of one screw sense over the other. As shown in Figure 1, the geometry optimized DFT model $(S,S)_3$-**2**, having (*S*)-chiral alcohol groups, adopted the (*M*)-helical structure as the most stable conformation, in which bulky phenyl groups pointed *away* from the sterically congested molecular core to alleviate steric crowding (Figure 1). On the other hand, the corresponding (*P*)-conformer with six phenyl groups pointing *toward* the center of the molecule was energetically disfavored by 12 kcal mol^{-1}. The mirror-image isomer $(R,R)_3$-**2** with (*R*)-chiral centers adopted the (*P*)-helical conformation which is enantiomeric to (*M*)-$(S,S)_3$-**2**, thereby establishing a direct transfer of carbon-centered chiral information to the helical screw sense of the dendritic molecular backbone.

Structural folding through hydrogen bonds brings into close proximity multiple chiral centers that are remote in the molecule's branched backbone. Molecular C_3-symmetry plays a pivotal role here by maximizing the number of pairwise contacts between bulky chiral groups and thereby effectively amplifying local steric bias. This stereoinduction model was subsequently tested for a homologous series of compounds with systematic variations made in the number as well as in the absolute configuration of the chiral centers.

Synthesis. As proof of principle, an enantiomeric pair of compounds $(R,R)_3$-**3** and $(S,S)_3$-**3** were prepared in a high-yielding (>90%) two-step synthesis using commercially available chiral alcohols (Scheme 2). As an isolated chiral arm model, (*S,S*)-**4** was prepared. Efficient cross-coupling protocols facilitated access to the chiral anilines **10** and **11**, which were subsequently incorporated into $(S)_3$-**5** and $(S)_3$-**6**. These com-

(9) (a) Chong, J. H.; Sauer, M.; Patrick, B. O.; MacLachlan, M. J. *Org. Lett.* **2003**, *5*, 3823–3826. (b) Sauer, M.; Yeung, C.; Chong, J. H.; Patrick, B. O.; MacLachlan, M. J. *J. Org. Chem.* **2006**, *71*, 775–788.
(10) (a) Yelamaggad, C. V.; Achalkumar, A. S.; Rao, D. S. S.; Prasad, S. K. *J. Am. Chem. Soc.* **2004**, *126*, 6506–6507. (b) Yelamaggad, C. V.; Achalkumar, A. S.; Rao, D. S. S.; Prasad, S. K. *J. Org. Chem.* **2007**, *72*, 8308–8318. (c) Yelamaggad, C. V.; Achalkumar, A. S.; Rao, D. S. S.; Prasad, S. K. *J. Mater. Chem.* **2007**, *17*, 4521–4529.
(11) (a) Riddle, J. A.; Bollinger, J. C.; Lee, D. *Angew. Chem., Int. Ed.* **2005**, *44*, 6689–6693. (b) Riddle, J. A.; Lathrop, S. P.; Bollinger, J. C.; Lee, D. *J. Am. Chem. Soc.* **2006**, *128*, 10986–10987. (c) Lim, Y.-K.; Wallace, S.; Bollinger, J. C.; Chen, X.; Lee, D. *Inorg. Chem.* **2007**, *46*, 1694–1703. (d) Jiang, X.; Bollinger, J. C.; Lee, D. *J. Am. Chem. Soc.* **2006**, *128*, 11732–11733. (e) Lim, Y.-K.; Jiang, X.; Bollinger, J. C.; Lee, D. *J. Mater. Chem.* **2007**, *17*, 1969–1980. (f) Jiang, X.; Vieweger, M. C.; Bollinger, J. C.; Dragnea, B.; Lee, D. *Org. Lett.* **2007**, *9*, 3579–3582. (g) Riddle, J. A.; Jiang, X.; Huffman, J.; Lee, D. *Angew. Chem., Int. Ed.* **2007**, *46*, 7019–7022.
(12) Opsitnick, E.; Lee, D. *Chem. Eur. J.* **2007**, *13*, 7040–7049.
(13) Riddle, J. A.; Jiang, X.; Lee, D. *Analyst* **2008**, *133*, 417–422.
(14) (a) Feringa, B. L.; van Delden, R. A.; Koumura, N.; Geertsema, E. M. *Chem. Rev.* **2000**, *100*, 1789–1816. (b) Feringa, B. L.; van Delden, R. A.; ter Wiel, M. K. J. In *Molecular Switches*; Feringa, B. L., Ed.; Wiley-VCH: Weinheim, 2001; pp 123−163. (c) Kay, E. R.; Leigh, D. A.; Zerbetto, F. *Angew. Chem., Int. Ed.* **2007**, *46*, 72–191.
(15) (a) Gilli, P.; Bertolasi, V.; Ferretti, V.; Gilli, G. *J. Am. Chem. Soc.* **2000**, *122*, 10405–10417. (b) Chin, J.; Kim, D. C.; Kim, H.-J.; Panosyan, F. B.; Kim, K. M. *Org. Lett.* **2004**, *6*, 2591–2593. (c) Sobczyk, L.; Grabowski, S. J.; Krygowski, T. M. *Chem. Rev.* **2005**, *105*, 3513–3560.

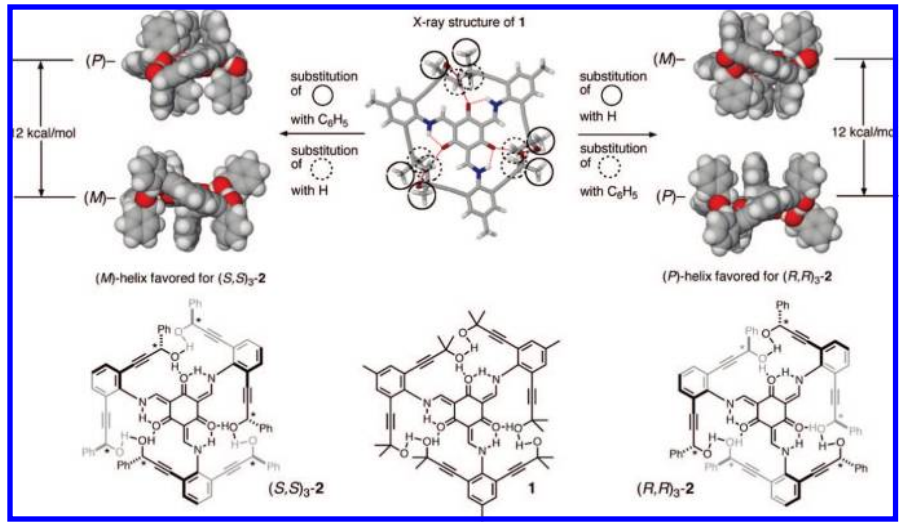

Figure 1. Capped-stick representation of the X-ray structure of **1** with O−H···O−H···O···H−N hydrogen-bonding network represented as red dotted lines,[11d] and space-filling representation of DFT models $(S,S)_3$-**2** and $(R,R)_3$-**2** constructed by formal asymmetric substitution of the *gem*-dimethyl groups of **1** (indicated by solid and dotted circles) with H and C_6H_5. The absolute screw sense, either (*P*)- or (*M*)-, of **2** is determined by the orientation of the three aniline rings that are unidirectionally tilted with respect to the molecular C_3-axis. For **1**, the (*P*)- and (*M*)-helixes are isoenergetic, for which only the (*M*)-isomer is shown here. See Scheme 1.

Scheme 2. Synthetic Routes to Chiral Tris(*N*-salicylideneaniline)s and *N*-Salicylideneaniline

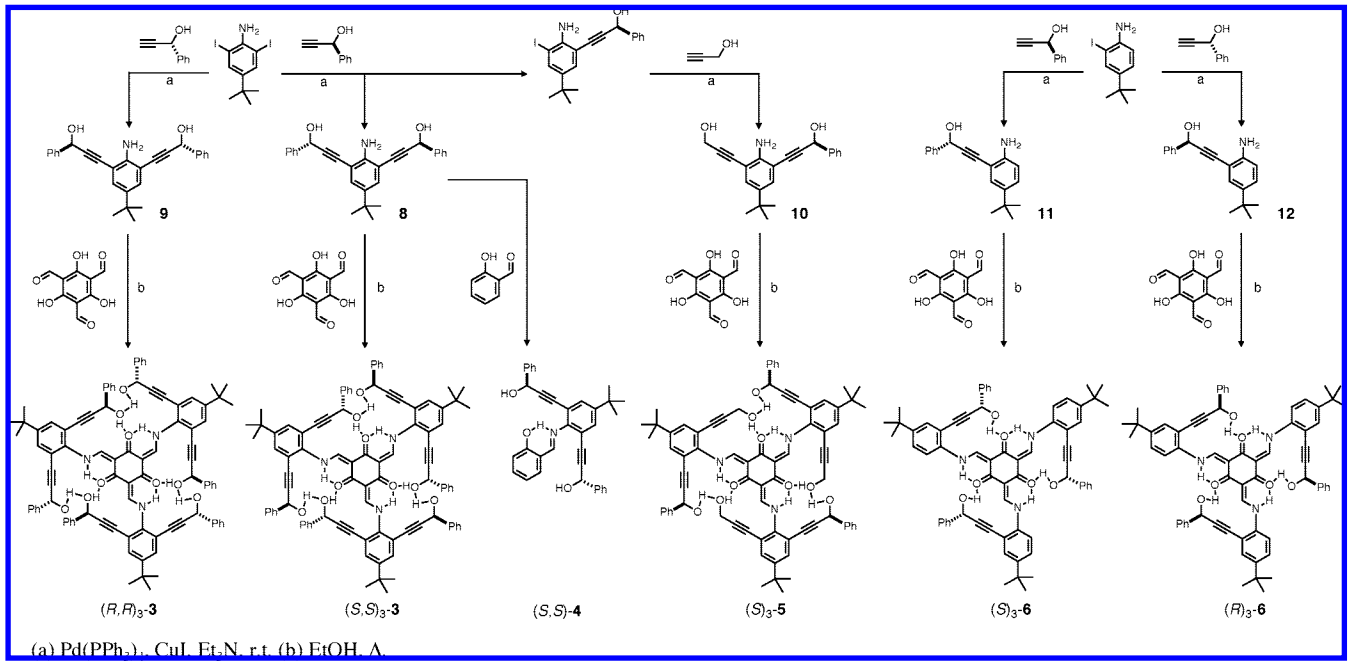

pounds were specifically designed in order to introduce variations in the number of hydrogen bonds and the number of chiral centers relative to $(S,S)_3$-**3**. The mirror-image isomer $(R)_3$-**6** was also prepared in a straightforward manner.

UV−vis and CD Spectroscopy. In $CHCl_3$ at 298 K, $(R,R)_3$-**3** and $(S,S)_3$-**3** displayed essentially identical UV−vis but displayed mirror-image CD spectra showing Cotton effects with opposite signs (Figure 2). Time-dependent (TD) DFT studies established that the longer-wavelength electronic transitions at $\lambda_{max} \approx 430$ nm of $(R,R)_3$- and $(S,S)_3$-**3** originate from molecular orbitals that are associated with peripheral aryl groups conjugated to the tris(*N*-salicylideneamine) molecular core. As shown by the frontier orbitals involved in the strong excitation of $(S,S)_3$-**2** at $\lambda_{max,calc} = 428$ nm (Figure 3 and Figure S1 [Supporting Information]), resonance-assisted hydrogen bonds[15] at the tris(*N*-salicylideneamine) core assist electronic conjugation between carbonyl and alkenyl groups and facilitate π-orbital overlap between the nitrogen lone pair electrons and the peripheral phenyl rings.

Quantitative predictions with TD-DFT further validated the assignment of absolute screw sense shown in Figure 1. Using the DFT model $(S,S)_3$-**2** (Figure 1), rotational strengths of the 60 lowest-energy electronic excitations were calculated and used to simulate the CD spectrum. As shown in Figure 4, the CD spectra of the (*M*)-helical conformer thus constructed using either BP86/TZP or LB94/TZP DFT functionals consistently predicted positive Cotton effects at >300 nm with intensity patterns similar to those experimentally observed for $(S,S)_3$-**3** (Figure 2).

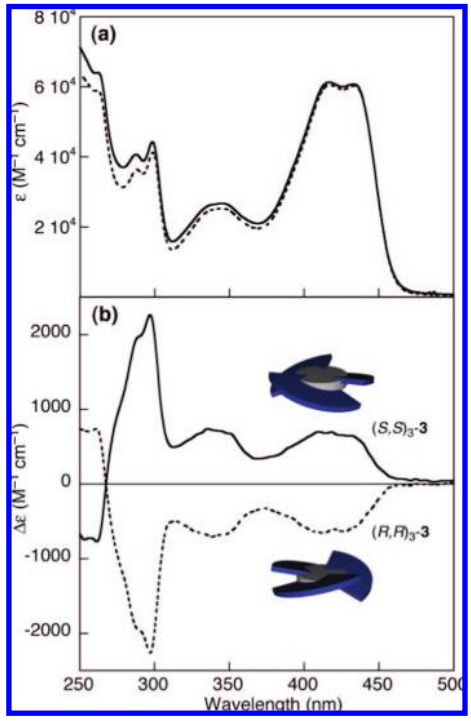

Figure 2. (a) UV−vis and (b) CD spectra of $(S,S)_3$-**3** (solid line) and $(R,R)_3$-**3** (dashed line) measured in $CHCl_3$ at 298 K.

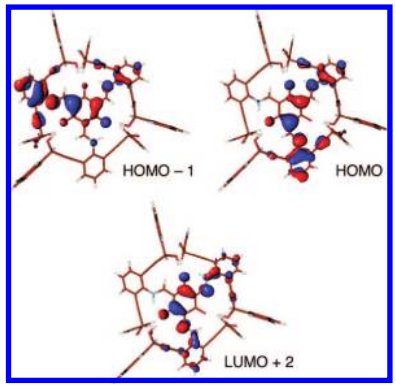

Figure 3. Isosurface plots (isodensity value = 0.035 au) of HOMO, HOMO−1, and LUMO+2 involved in the strong excitation at $\lambda_{max,calc}$ = 428 nm of $(S,S)_3$-**2**.

As indicated by the frontier molecular orbital (FMO) plots shown in Figure 3, a significant delocalization of electron densities over the helically twisted molecular backbone is responsible for the strong ($\Delta\varepsilon = 650-700\ M^{-1}\ cm^{-1}$) positive CD band observed for $(S,S)_3$-**2** at $\lambda \approx 430$ nm. In support of this notion, the CD spectrum of the isolated chiral arm model (*S,S*)-**4** (Scheme 2) showed only weak ($\Delta\varepsilon < 300\ M^{-1}\ cm^{-1}$) signal at $\lambda < 285$ nm with no features found in the longer wavelength region (Figure 5).

As shown in Figure 5, a homologous series of compounds $(S,S)_3$-**3**, $(S)_3$-**5**, and $(S)_3$-**6**, all built with identical chiral alcohol fragments, consistently showed positive Cotton effects in the longer wavelength, thereby establishing a direct correlation between the handedness of helical folding and the absolute configuration of carbon-centered chirality. This trend is maintained regardless of the number of chiral centers such as $(S,S)_3$-**3** vs $(S)_3$-**5** and $(S)_3$-**6**, or the number of alcohol groups such as $(S)_3$-**5** vs $(S)_3$-**6**.

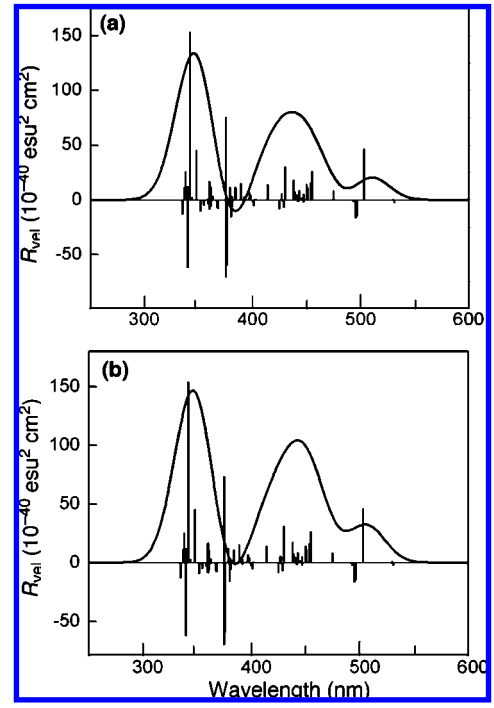

Figure 4. CD spectrum of $(S,S)_3$-**2** calculated using DFT functionals (a) BP86/TZP or (b) LB94/TZP. Vertical lines indicate rotatory strengths. The spectrum was constructed using the Gaussian convolution and scaled by empirically adjusting the linewidths.

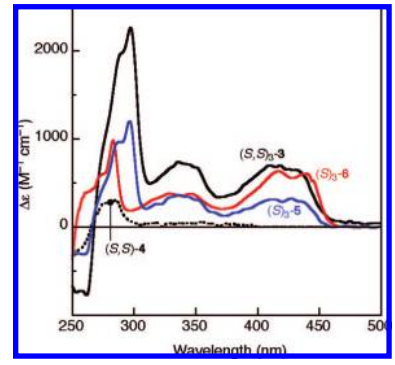

Figure 5. CD spectra of chiral tris(*N*-salicylideneaniline)s and *N*-salicylideneaniline measured in $CHCl_3$ at 298 K.

1D and 2D ^{1}H NMR Studies: Hydrogen-Bonding Assisted Structural Folding. In $CDCl_3$ at 298 K, compounds $(S,S)_3$-**3**, $(S)_3$-**5**, and $(S)_3$-**6** showed coupled ($J = 13.2$ Hz) N−H and C−H doublets at 14.01−13.34 and 9.64−8.78 ppm, respectively. These features are in agreement with the keto-enamine, rather than enol-imine, tautomer description of the tris(*N*-salicylideneamine) core.[9a] Notably, the simple spectral patterns with only one set of $N_{enamine}$−H and C_{vinyl}−H proton resonances indicated exclusive formation of only one isomer of C_3-symmetry.[11] The significantly downfield-shifted OH proton resonances (5.24−6.25 ppm) of these compounds relative to that (3.05 ppm) of (*S,S*)-**4** indicated hydrogen-bonding interactions involving wing-tip alcohol groups,[11d,e,g] which prompted a further investigation of solution structures.

The 2D-ROESY ^{1}H NMR spectrum of $(S)_3$-**5** in $CDCl_3$ (Figure 6a) revealed multiple cross-peaks associated with the ethynyl-extended alcohol groups and the enamine skeleton at the molecular core which are brought in close proximity through structural folding. A strong ROE correlation between the two

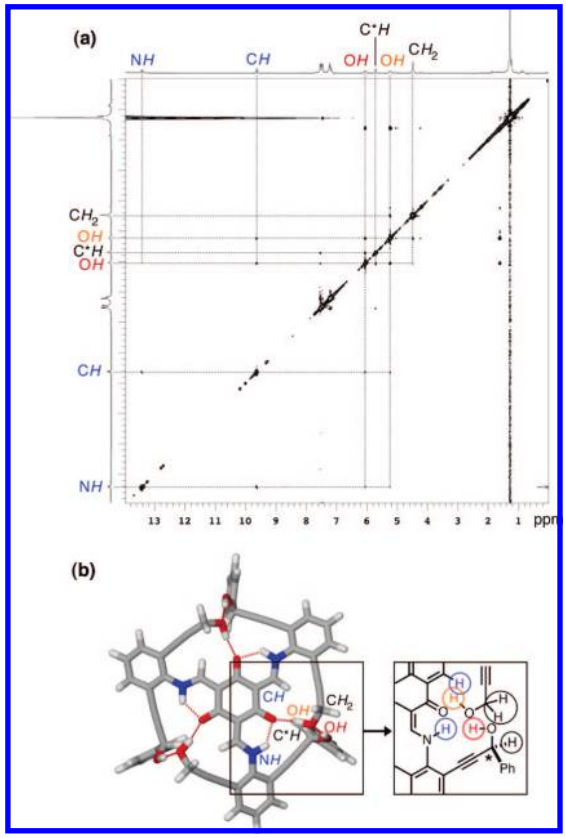

Figure 6. (a) 2D ROESY spectrum of $(S)_3$-**5** in $CDCl_3$ solution at T = 298 K. (b) Capped-stick representation of the DFT geometry optimized model of $(S)_3$-**5** showing protons contributing to ROE and TOCSY-relayed ROE cross peaks. Red dotted lines indicate hydrogen bonds. The *tert*-butyl groups on the aniline rings have been omitted for clarity. A close-up view of the chemical structure is shown next.

alcohol OH protons was indeed in agreement with the relatively short O···O interatomic distance of ~2.37 Å determined from the DFT geometry optimized model (Figure 6b). In addition, the OH−OH cross peaks have an opposite phase with respect to those of CH−OH and NH−OH, which is consistent with chemical exchange through O−H···O−H contacts that are maintained in solution.[16] Collectively, these findings provided compelling evidence that helical folding through the formation of a cyclic hydrogen-bonding network, previously seen in crystal structures,[11e,f] is an intrinsic propensity of the molecule, not an artifact of solid-state packing interactions.

Energetics of Structural Folding and Unfolding: Temperature-Dependent Studies. A reversible assembly and disassembly of the hydrogen-bonding network can drive structural folding and unfolding. The cooperative nature[2,17] of this process could be approximated by a simple two-state model (Scheme 3). The "all-or-nothing" behavior of the molecule in this idealized situation approaches a genuine switch,[11g,13,18] which can be operated by change in the temperature.

The single OH proton resonance experimentally observed in the ^{1}H NMR spectrum of $(S,S)_3$-**3** indicated a fast exchange in solution to provide a population averaged δ_{obs} value. With the

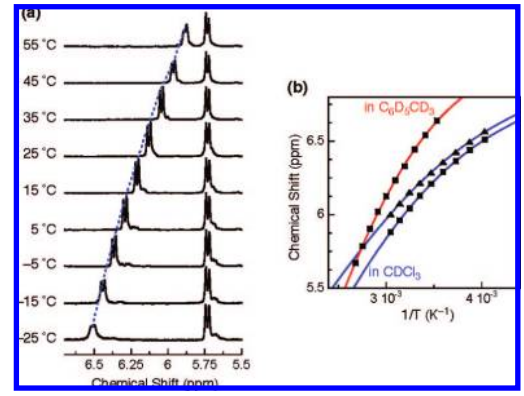

Figure 7. (a) ^{1}H NMR spectra (400 MHz) of $(S,S)_3$-**3** in $CDCl_3$ showing shifts of OH proton resonances as a function of temperature from −25 to +55 °C. (b) Plots of δ_{obs} vs $1/T$. Measured data points are denoted by square markers for $(S,S)_3$-**3** and triangular markers for $(S)_3$-**6**. Fits to the data by the model are delineated by red (in toluene-d_8) and blue (in $CDCl_3$) curves. See text for the thermodynamic parameters, ΔH and ΔS, derived from nonlinear curve fitting.

Scheme 3. Binary Switching between the Folded (A) and Unfolded (B) Conformer through the Assembly (←) and Disassembly (→) of the Hydrogen-Bonding Network

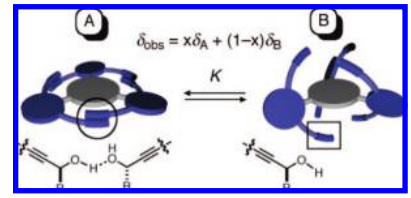

switching model shown in Scheme 3, this observable can be deconvoluted into contributions from the folded **A** (δ_A) and unfolded **B** (δ_B) conformers which exist in mole fractions of x and $1 - x$, respectively. A systematic downfield shift of δ_{obs} with decreasing temperature (Figure 7) indicated an equilibrium shift toward **A** with hydrogen-bonding-induced deshielding of the O−H protons. In addition, the slower exchange kinetics at lower temperature apparently led to significant line broadening. These VT ^{1}H NMR data were subsequently analyzed using eq 1 in order to derive the ΔH and ΔS parameters dictating the thermodynamics of structural folding and unfolding.

$$\delta_{obs} = (\delta_A - \delta_B)\left[\exp\left\{-\frac{\Delta H}{R}\left(\frac{1}{T}\right) + \frac{\Delta S}{R}\right\} + 1\right]^{-1} + \delta_B \qquad (1)$$

Initial fitting of the data obtained for $(S,S)_3$-**3** in $CDCl_3$ within the temperature range 248−328 K provided δ_B = 2.28 ppm as the OH proton resonance of the unfolded conformer **B**. This value was close to the OH proton resonance at 2.35 ppm experimentally determined for the free amine compound **8** (T = 298 K), and thus supported the validity of our simplified two-state model (Scheme 3). A nonlinear regression of the δ_{obs} vs $1/T$ data (Figure 7b) with δ_B fixed at 2.35 ppm furnished δ_A = 6.94 ± 0.02 ppm, ΔH = 2.2 ± 0.1 kcal mol^{-1}, and ΔS = 4.2 ± 0.1 cal mol^{-1} K^{-1}. Comparable thermodynamic parameters were obtained for $(S,S)_3$-**3** in toluene-d_8 with ΔH = 3.0 ± 0.1 kcal mol^{-1} and ΔS = 6.4 ± 0.3 cal mol^{-1} K^{-1}, and for $(S)_3$-**6** in $CDCl_3$ with ΔH = 2.0 ± 0.1 kcal mol^{-1} and ΔS = 4.2 ± 0.2 cal mol^{-1} K^{-1} (Figure 7), all consistently pointing toward the endothermic nature of structural unfolding with positive change in entropy.

Solvent-Induced Helicity Inversion. Solvent−solute interactions profoundly affect the stability of conformationally flexible

(16) Neuhaus, D.; Williamson, M. P. *The Nuclear Overhauser Effect in Structural and Conformational Analysis*, 2nd ed.; Wiley-VCH: New York, 2000.
(17) Whitty, A. *Nat. Chem. Biol.* **2008**, *4*, 435–439.
(18) Shinkai, S.; Ikeda, M.; Sugasaki, A.; Takeuchi, M. *Acc. Chem. Res.* **2001**, *34*, 494–503.

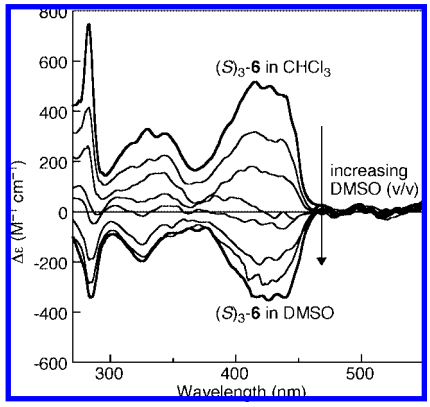

Figure 8. Changes in the CD spectrum of $(S)_3$-**6** with increasing volume fraction of DMSO in $CHCl_3$−DMSO mixed solvents at 298 K. $CHCl_3$/DMSO (v/v) = 100:0, 90:10, 80:20, 70:30, 60:40, 40:60, 20:80, and 0:100 from top to bottom trace.

molecules and their higher-order assemblies.[4,5,19−21] With VT ^{1}H NMR studies providing valuable insights into structural folding and unfolding of $(S)_3$-**6**, we initiated investigating the feasibility of using molecule−solvent interactions to drive a similar process. We reasoned that strong hydrogen-bond acceptor solvents would disrupt the O−H···O hydrogen-bonding network to trigger conformational transitions that can be monitored directly.

As anticipated, the CD spectrum of $(S)_3$-**6** gradually lost the intensity of its positive band with increasing volume fraction of DMSO in $CHCl_3$−DMSO mixed-solvent system and became essentially featureless between 30 and 40% DMSO (v/v) at 298 K (Figure 8). Contrary to our intuitive prediction, however, a further increase in the volume fraction of DMSO above this critical ratio elicited an apparent "refolding" of the structure to opposite helicity. This striking behavior was most effectively demonstrated by the CD spectrum of $(S)_3$-**6** measured in 100% DMSO, which displayed a *pseudo* mirror-image relationship to that taken in 100% $CHCl_3$ (Figure 8). Under identical conditions, $(R)_3$-**6** showed an exactly opposite behavior, with negative-to-positive sign change in Cotton effects upon changing solvent from $CHCl_3$ to DMSO (Figure S2 [Supporting Information]). A similar solvent-dependent helicity inversion was observed also for $(S,S)_3$-**3** or $(R,R)_3$-**3**, although the magnitude of the Cotton effects with reversed sign was smaller than that of $(S)_3$-**6** or $(R)_3$-**6**.

The UV−vis spectra of $(S)_3$-**6** in $CHCl_3$-DMSO obtained with varying volume ratio remained essentially invariant (Figure S1 [Supporting Information]), thus making aggregation or other intermolecular interactions a less likely source for the experimentally observed CD sign change. Chiral aggregation typically accompanies evolution of exciton-coupled circular dichroism (ECCD) from interchromophore interactions,[22−24] which was not observed in our case.

The 1-D and 2-D ^{1}H NMR spectrum of $(S)_3$-**6** in DMSO-d_6 showed a significant broadening of OH proton resonances and

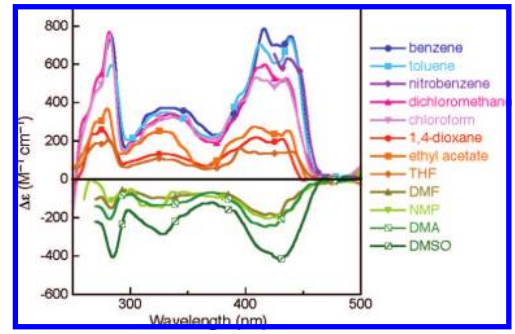

Figure 9. Solvent-dependent changes in the CD spectrum of $(S)_3$-**6** measured in benzene, toluene, nitrobenzene, dichloromethane, chloroform, 1,4-dioxane, ethyl acetate, THF, DMF, NMP, DMA, and DMSO at T = 298 K. Due to strong solvent absorption, data in nitrobenzene was obtained only for >420 nm.

lack of correlated peaks, indicating disassembly of the O−H···O hydrogen-bonding network as a consequence of rapid chemical exchange with solvent molecules. The loss of critical anchoring contacts between the wing-tip OH groups and the core carbonyl groups might trigger the experimentally observed solvent-induced helicity switching. Alternatively, a preferential stabilization of one screw sense over the other can be envisioned if the molecule experiences a substantial change in solvent-accessible surface upon structural unfolding and refolding. A significant change in solvent dielectric from $CHCl_3$ (ε = 4.89) to DMSO (ε = 46.45)[19] could enforce the molecule to adopt opposite helicity in order to minimize contact between its poorly solvated nonpolar aromatic surfaces and polar environment.[21]

Correlation with Solvent Parameters. In order to obtain a better understanding of the role of solvents in helicity inversion, the CD spectra of $(S)_3$-**6** were obtained in 12 different solvents with varying degrees of polarity and hydrogen-bonding donor/acceptor ability. As shown in Figure 9, $(S)_3$-**6** displayed strong positive Cotton effects in benzene, toluene, nitrobenzene, CH_2Cl_2, and $CHCl_3$. The intensity of the positive band became significantly diminished in 1,4-dioxane, ethyl acetate, and THF and eventually reversed its sign in DMF, NMP, DMA, and DMSO solution samples. The sign and magnitude of the CD signal at 430 nm, $\Delta\varepsilon_{430}$, reflect the absolute screw sense and stability of helical folding in this system and thus served as a convenient experimental observable in our subsequent analysis.

The effect of solvent on structural folding was investigated by plotting $\Delta\varepsilon_{430}$ of $(S)_3$-**6** against selected solvent parameters. As shown in Figure 10, good correlations were observed between $\Delta\varepsilon_{430}$ and donor number (DN),[19,25,26] as a measure of Lewis basicity, or solvent basicity (SB),[19,17] as a measure of

(19) Reichardt, C. *Solvents and Solvent Effects in Organic Chemistry*, 3rd ed.; Wiley-VCH: Weinheim, 2003.
(20) Zhao, Y.; Zhong, Z.; Ryu, E.-H. *J. Am. Chem. Soc.* **2007**, *129*, 218–225.
(21) Zhao, Y.; Moore, J. S. In *Foldamers*; Hecht, S., Huc, I., Eds.; Wiley-VCH: Weinheim, 2007; pp 75−108.
(22) *Circular Dichroism: Principles and Applications*, 2nd ed.; Berova, N.; Nakanishi, K., Woody, R. W., Eds.; VCH: New York, 2000.
(23) Würthner, F., Ed. *Supramolecular Dye Chemistry*; Springer-Verlag: Berlin, Germany, 2005.
(24) (a) Imada, T.; Murakami, H.; Shinkai, S. *J. Chem. Soc., Chem. Commun.* **1994**, 1557–1558. (b) Kilbinger, A. F. M.; Schenning, A. P. H. J.; Goldoni, F.; Feast, W. J.; Meijer, E. W. *J. Am. Chem. Soc.* **2000**, *122*, 1820–1821. (c) Zsila, F.; Bikádi, Z.; Keresztes, Z.; Deli, J.; Simonyi, M. *J. Phys. Chem. B* **2001**, *105*, 9413–9421. (d) Morikawa, M.-a.; Yoshihara, M.; Endo, T.; Kimizuka, N. *J. Am. Chem. Soc.* **2005**, *127*, 1358–1359. (e) Spano, F. C.; Meskers, S. C. J.; Hennebicq, E.; Beljonne, D. *J. Am. Chem. Soc.* **2007**, *129*, 7044–7054. (f) Seibt, J.; Lohr, A.; Würthner, F.; Engel, V. *Phys. Chem. Chem. Phys.* **2007**, *9*, 6214–6218. (g) Xiao, J.; Xu, J.; Cui, S.; Liu, H.; Wang, S.; Li, Y. *Org. Lett.* **2008**, *10*, 645–648.
(25) (a) Gutmann, V. *Coord. Chem. Rev.* **1967**, *2*, 239–256. (b) Gutmann, V. *Coord. Chem. Rev.* **1976**, *18*, 225–255. (c) Linert, W.; Fukuda, Y.; Camard, A. *Coord. Chem. Rev.* **2001**, *218*, 113–152.
(26) DN_λ estimated from spectral data of solvatochromic indicators was used instead of DN for toluene, CH_2Cl_2, and $CHCl_3$.[25c]
(27) Catalán, J. In *Handbook of Solvents*; Wypych, G., Ed.; ChemTec Publishing: Toronto, 2001.

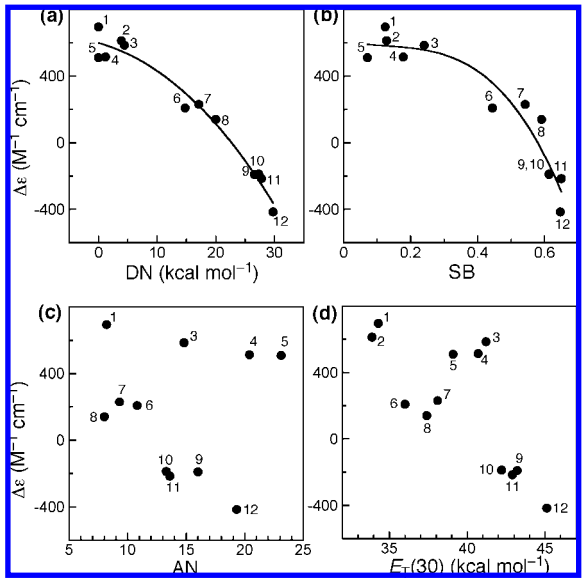

Figure 10. Plots of $\Delta\varepsilon_{430}$ (=$\Delta\varepsilon$ at 430 nm in M^{-1} cm^{-1}) of $(S)_3$-**6** vs (a) donor number (DN), (b) solvent basicity (SB), (c) acceptor number (AN), or (d) $E_T(30)$ for solvents including benzene (1), toluene (2), nitrobenzene (3), dichloromethane (4), chloroform (5), 1,4-dioxane (6), ethyl acetate (7), THF (8), DMF (9), NMP (10), DMA (11), and DMSO (12).

hydrogen-bond acceptor ability. In contrast, plots of $\Delta\varepsilon_{430}$ vs acceptor number (AN),[19,28] as a measure of Lewis acidity, or $E_T(30)$,[19,29] as a measure of solvent polarity, showed scattered data points with no remarkable trends. These empirical findings suggest that solvent, instead of functioning as a simple macroscopic continuum exerting nondirectional forces, actively participates in specific O−H···solvent interactions to drive structural unfolding and eventual helicity inversion.[30] A conceptually related mechanistic model was previously considered for dipyrrinone derivatives that changed Cotton effect signs upon changing solvent from CH_2Cl_2 to DMSO[31] or addition of amine cosolvents.[32] It was proposed that the steric constraints imposed by strong N−H···O═S$(CH_3)_2$ hydrogen bonds or carboxylate··· ammonium salt bridges trigger conformational twisting and reorientation of the electronic transition dipoles.

Covalently-Triggered Helicity Inversion. A detailed mechanistic understanding of this intriguing helicity switching awaits precise solution structure analysis. We reasoned, however, that chemical modification of the OH groups in $(S)_3$-**6** to simulate solvent-induced disruption of the O−H···O hydrogen-bonding network could have essentially identical consequences in structural dynamics.

This idea was tested in a straightforward manner using $(S)_3$-**7**, in which all the OH groups in $(S)_3$-**6** were protected with TMS groups to mimic the O−H···solvent interactions. In CH_2Cl_2 at 298 K, $(S)_3$-**7** indeed displayed a negative Cotton effect (Figure 11), similarly to the behavior of $(S)_3$-**6** in DMSO (Figure 8). A facile protiodesilylation of $(S)_3$-**7** with 10 equiv of TBAF at room temperature, however, induced helicity switching. As shown in Figure 11, the CD spectrum of the final

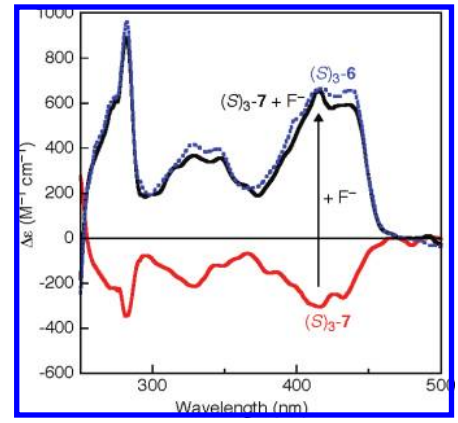

Figure 11. CD spectra of $(S)_3$-**7** in CH_2Cl_2 doped with H_2O (0.1%, v/v) measured prior to (red, solid line) and 30 min after (black, solid line) addition of Bu_4NF (10 equiv) at 298 K. The CD spectrum of $(S)_3$-**6** (blue, dotted line) measured under identical conditions is shown for comparison.

Scheme 4. Covalently-Driven Helicity Switching Cycle

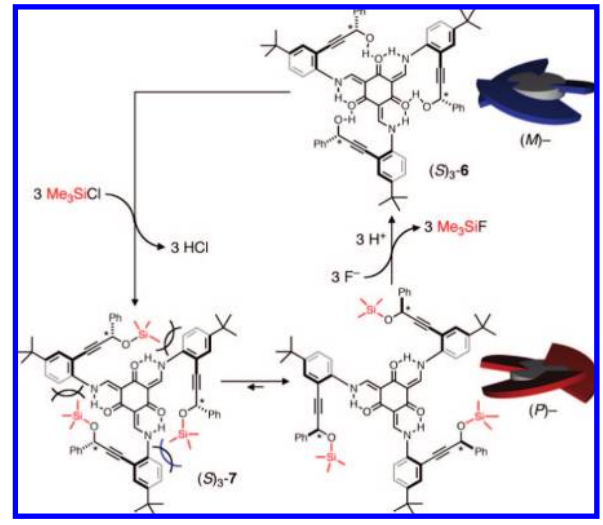

reaction product was essentially superimposable on that of $(S)_3$-**6**. An HPLC analysis of the reaction mixture established quantitative formation of $(S)_3$-**6**.

One mechanistic model that is consistent with this experimental observation is shown in Scheme 4, in which $(S)_3$-**7** adopts a (*P*)-helical conformation in order to alleviate steric constraints imposed by the bulky TMS wing-tip groups. Desilylation by F^- and subsequent protonation furnishes $(S)_3$-**6** and restores the key O−H···O network stabilizing the (*M*)-conformer to formally complete the helicity switching cycle.

Summary and Outlook. Steric interactions between neighboring branches can collectively determine the screw sense of helically folding dendritic molecules. This idea was implemented with a series of C_3-symmetric tris(*N*-salicylideneaniline)s having chiral alcohol groups strategically placed around a cyclic hydrogen-bonding network. Reversible assembly and disas-

(28) (a) Mayer, U.; Gutmann, V.; Gerger, W. *Monatsh. Chem.* **1975**, *106*, 1235–1257. (b) Mayer, U.; Gerger, W.; Gutmann, V. *Monatsh. Chem.* **1977**, *108*, 489–498. (c) Mayer, U. *Pure Appl. Chem.* **1979**, *51*, 1697–1712.
(29) Reichardt, C. *Chem. Rev.* **1994**, *94*, 2319–2358.
(30) Johnson, R. S.; Yamazaki, T.; Kovalenko, A.; Fenniri, H. *J. Am. Chem. Soc.* **2007**, *129*, 5735–5743.
(31) Byun, Y.-S.; Lightner, D. A. *J. Org. Chem.* **1991**, *56*, 6027–6033.
(32) Boiadjiev, S. E.; Lightner, D. A. *J. Am. Chem. Soc.* **2000**, *122*, 378–383.
(33) Fenniri, H.; Deng, B.-L.; Ribbe, A. E. *J. Am. Chem. Soc.* **2002**, *124*, 11064–11072.
(34) Lohr, A.; Lysetska, M.; Würthner, F. *Angew. Chem., Int. Ed.* **2005**, *44*, 5071–5074.
(35) Palmans, A. R. A.; Meijer, E. W. *Angew. Chem., Int. Ed.* **2007**, *46*, 8948–8968, and references cited therein.

sembly of this key *chirality transfer channel* induced a highly unusual helicity switching.

Chirality inversion has previously been observed for supramolecular aggregates,[30,33−35] polymers,[14a,36−44] and foldamers[45−50] in which cooperative noncovalent interactions lead to an effective amplification of locally introduced steric bias. For small molecule systems with a limited number of weak bonds to manipulate, chirality switching becomes a significant challenge. Several small molecule systems do exist, however, which undergo reversal in screw sense through photochemically driven isomerization around a sterically overcrowded double bond,[14a,51] redox-[52] or coordination-driven[53−55] rearrangement of primary metal coordination sphere, or solvent-induced chirality inversion of dendrons,[56] bis(porphyrin) tweezers,[57] dipyrrinone derivatives,[32] or biaryl rotors.[58]

Our findings described in this paper suggest that covalently triggered conformational transition can be a viable strategy to achieve helicity inversion of stereodynamic small molecules. Efforts are currently underway to unravel the molecular basis of this intriguing phenomenon and to find technological applications of this emerging class of chiral switches.

Experimental Section

General Considerations. All reagents were obtained from commercial suppliers and used as received unless otherwise noted. THF was saturated with nitrogen and purified by passage through activated Al_2O_3 columns under nitrogen (Innovative Technology SPS 400). Triethylamine was saturated with nitrogen and used without further purification. Trimethylsilyl chloride was distilled over CaH_2 and stored under nitrogen. The compounds 1,3,5-triformylphloroglucinol,[9a] 2-iodo-4-*tert*-butylaniline, and 2,6-diiodo-4-*tert*-butylaniline[59] were prepared according to literature procedures. All air-sensitive manipulations were carried out under nitrogen atmosphere in an M.Braun glovebox or by standard Schlenk-line techniques.

Physical Measurements. ^{1}H NMR and ^{13}C NMR spectra were recorded on a 400 MHz Varian Inova NMR Spectrometer. Chemical shifts were reported versus tetramethylsilane and referenced to the residual solvent peaks. High resolution chemical ionization (CI) (using CH_4 as CI reagent) and electrospray ionization (ESI) mass spectra were obtained on a Thermo Electron Corporation MAT 95XP-Trap. FT-IR spectra were recorded on a Nicolet Avatar 360 FT-IR Spectrometer with EZ OMNIC ESP software. UV−vis spectra were recorded on a Varian Cary 5000 UV−vis−NIR spectrophotometer. Circular dichroism (CD) spectra were collected on a Jasco J-715 circular dichroism spectropolarimeter. HPLC analyses were carried out on a Waters Breeze HPLC System using a chiral column (Regis Technologies Inc., Pirkle Covalent (*S,S*)-Whelk-O 1 10/100 FEC, o.d. 0.46 cm × 25 cm).

Reactions with Fluoride Ion. Stock solutions of tetrabutylammonium fluoride (TBAF) were prepared using TBAF·3H_2O and anhydrous THF in the glovebox. Sample solutions of $(S)_3$-**6** and $(S)_3$-**7** were prepared with CH_2Cl_2 doped with H_2O (0.1%, v/v). In order to minimize dilution effects, 10 μL aliquots of TBAF solutions were delivered to sample solutions of $(S)_3$-**6** or $(S)_3$-**7** (3.5 mL) using microsyringes prior to measurements.

(1*S*,1′*S*)-3,3′-(2-Amino-5-*tert*-butyl-1,3-phenylene)bis(1-phenylprop-2-yn-1-ol) (8). A round-bottom flask was charged with 4-*tert*-butyl-2,6-diiodoaniline (1.03 g, 2.58 mmol), (*R*)-1-phenyl-2-propyn-1-ol (750 mg, 5.67 mmol), Et_3N (20 mL), $Pd(PPh_3)_4$ (60 mg, 0.052 mmol), and CuI (15 mg, 0.079 mmol) at room temperature. The reaction mixture was purged with N_2, stirred for 24 h at rt, and concentrated under reduced pressure. Flash column chromatography on SiO_2 (hexanes/EtOAc = 3:2, v/v) furnished **8** as a yellow solid (1.05 g, 2.56 mmol, 99%). ^{1}H NMR (400 MHz, $CDCl_3$, 298 K): δ 7.62−7.55 (m, 4H), 7.41−7.33 (m, 6H), 7.32 (s, 2H), 5.75 (d, J = 5.6 Hz, 2H), 4.59 (bs, 2H), 2.35 (d, J = 6.0 Hz, 2H), 1.25 (s, 9H);

(36) (a) For reviews, see: Yashima, E.; Maeda, K.; Nishimura, T. *Chem. Eur. J.* **2004**, *10*, 42–51. (b) Maeda, K.; Yashima, E. *Top. Curr. Chem.* **2006**, *265*, 47–88. (c) Yashima, E.; Maeda, K. In *Foldamers*; Hecht, S., Huc, I., Eds.; Wiley-VCH: Weinheim, 2007; pp 331−363. (d) Yashima, E.; Maeda, K. *Macromolecules* **2008**, *41*, 3–12.

(37) (a) Bouman, M. M.; Meijer, E. W. *Adv. Mater.* **1995**, *7*, 385–387. (b) Langeveld-Voss, B. M. W.; Christiaans, M. P. T.; Janssen, R. A. J.; Meijer, E. W. *Macromolecules* **1998**, *31*, 6702–6704.

(38) (a) Nakashima, H.; Fujiki, M.; Koe, J. R.; Motonaga, M. *J. Am. Chem. Soc.* **2001**, *123*, 1963–1969. (b) Nakashima, H.; Koe, J. R.; Torimitsu, K.; Fujiki, M. *J. Am. Chem. Soc.* **2001**, *123*, 4847–4848. (c) Fujiki, M.; Koe, J. R.; Motonaga, M.; Nakashima, H.; Terao, K.; Teramoto, A. *J. Am. Chem. Soc.* **2001**, *123*, 6253–6261.

(39) (a) Yashima, E.; Matsushima, T.; Okamoto, Y. *J. Am. Chem. Soc.* **1997**, *119*, 6345–6359. (b) Yashima, E.; Maeda, Y.; Okamoto, Y. *J. Am. Chem. Soc.* **1998**, *120*, 8895–8896. (c) Yashima, E.; Maeda, K.; Sato, O. *J. Am. Chem. Soc.* **2001**, *123*, 8159–8160. (d) Nonokawa, R.; Yashima, E. *J. Am. Chem. Soc.* **2003**, *125*, 1278–1283. (e) Maeda, K.; Morino, K.; Okamoto, Y.; Sato, T.; Yashima, E. *J. Am. Chem. Soc.* **2004**, *126*, 4329–4342. (f) Sakurai, S.-i.; Okoshi, K.; Kumaki, J.; Yashima, E. *J. Am. Chem. Soc.* **2006**, *128*, 5650–5651. (g) Maeda, K.; Mochizuki, H.; Watanabe, M.; Yashima, E. *J. Am. Chem. Soc.* **2006**, *128*, 7639–7650. (h) Okoshi, K.; Sakurai, S.-i.; Ohsawa, S.; Kumaki, J.; Yashima, E. *Angew. Chem., Int. Ed.* **2006**, *45*, 8173–8176.

(40) Tang, H.-Z.; Boyle, P. D.; Novak, B. M. *J. Am. Chem. Soc.* **2005**, *127*, 2136–2142.

(41) (a) Pijper, D.; Feringa, B. L. *Angew. Chem., Int. Ed.* **2007**, *46*, 3693–3696. (b) Pijper, D.; Jongejan, M. G. M.; Meetsma, A.; Feringa, B. L. *J. Am. Chem. Soc.* **2008**, *130*, 4541–4552.

(42) (a) Inouye, M.; Waki, M.; Abe, H. *J. Am. Chem. Soc.* **2004**, *126*, 2022–2027. (b) Abe, H.; Masuda, N.; Waki, M.; Inouye, M. *J. Am. Chem. Soc.* **2005**, *127*, 16189–16196. (c) Waki, M.; Abe, H.; Inouye, M. *Angew. Chem., Int. Ed.* **2007**, *46*, 3059–3061.

(43) (a) Cheuk, K. K. L.; Lam, J. W. Y.; Lai, L. M.; Dong, Y.; Tang, B. Z. *Macromolecules* **2003**, *36*, 9752–9762. (b) Lam, J. W. Y.; Tang, B. Z. *Acc. Chem. Res.* **2005**, *38*, 745–754.

(44) Satrijo, A.; Meskers, S. C. J.; Swager, T. M. *J. Am. Chem. Soc.* **2006**, *128*, 9030–9031.

(45) (a) Inai, Y.; Tagawa, K.; Takasu, A.; Hirabayashi, T.; Oshikawa, T.; Yamashita, M. *J. Am. Chem. Soc.* **2000**, *122*, 11731–11732. (b) Inai, Y.; Ousaka, N.; Okabe, T. *J. Am. Chem. Soc.* **2003**, *125*, 8151–8162.

(46) (a) Jiang, H.; Dolain, C.; Léger, J.-M.; Gornitzka, H.; Huc, I. *J. Am. Chem. Soc.* **2004**, *126*, 1034–1035. (b) Dolain, C.; Léger, J.-M.; Delsuc, N.; Gornitzka, H.; Huc, I. *Proc. Natl. Acad. Sci. U.S.A.* **2005**, *102*, 16146–16151. (c) Maurizot, V.; Dolain, C.; Huc, I. *Eur. J. Org. Chem.* **2005**, 1293–1301. (d) Dolain, C.; Jiang, H.; Léger, J.-M.; Guionneau, P.; Huc, I. *J. Am. Chem. Soc.* **2005**, *127*, 12943–12951.

(47) Prince, R. B.; Barnes, S. A.; Moore, J. S. *J. Am. Chem. Soc.* **2000**, *122*, 2758–2762.

(48) Hou, J.-L.; Yi, H.-P.; Shao, X.-B.; Li, C.; Wu, Z.-Q.; Jiang, X.-K.; Wu, L.-Z.; Tung, C.-H.; Li, Z.-T. *Angew. Chem., Int. Ed.* **2006**, *45*, 796–800.

(49) Ikeda, C.; Yoon, Z. S.; Park, M.; Inoue, H.; Kim, D.; Osuka, A. *J. Am. Chem. Soc.* **2005**, *127*, 534–535.

(50) Meudtner, R. M.; Hecht, S. *Angew. Chem., Int. Ed.* **2008**, *47*, 4926–4930.

(51) (a) Feringa, B. L.; Jager, W. F.; de Lange, B.; Meijer, E. W. *J. Am. Chem. Soc.* **1991**, *113*, 5468–5470. (b) Jager, W. F.; de Jong, J. C.; de Lange, B.; Huck, N. P. M.; Meetsma, A.; Feringa, B. L. *Angew. Chem., Int. Ed.* **1995**, *34*, 348–350. (c) Feringa, B. L. *Acc. Chem. Res.* **2001**, *34*, 504–513.

(52) (a) Zahn, S.; Canary, J. W. *Science* **2000**, *288*, 1404–1407. (b) Barcena, H. S.; Holmes, A. E.; Zahn, S.; Canary, J. W. *Org. Lett.* **2003**, *5*, 709–711. (c) Barcena, H. S.; Liu, B.; Mirkin, M. V.; Canary, J. W. *Inorg. Chem.* **2005**, *44*, 7652–7660.

(53) (a) Miyake, H.; Yoshida, K.; Sugimoto, H.; Tsukube, H. *J. Am. Chem. Soc.* **2004**, 6524–6525. (b) Miyake, H.; Sugimoto, H.; Tamiaki, H.; Tsukube, H. *Chem. Commun.* **2005**, 4291–4293.

(54) Hutin, M.; Nitschke, J. *Chem. Commun.* **2006**, 1724–1726.

(55) Gregolinski, J.; Slepokura, K.; Lisowski, J. *Inorg. Chem.* **2007**, *46*, 7923–7934.

(56) Hofacker, A. L.; Parquette, J. R. *Angew. Chem., Int. Ed.* **2005**, *44*, 1053–1057.

(57) Victor, V.; Borovkov; Hembury, G. A.; Inoue, Y. *Angew. Chem., Int. Ed.* **2003**, *42*, 5310–5314.

(58) Reichert, S.; Breit, B. *Org. Lett.* **2007**, *9*, 899–902.

(59) Iskra, J.; Stavber, S.; Zupan, M. *Synthesis* **2004**, 1869–1873.

^{13}C NMR (100 MHz, $CDCl_3$, 298 K): δ 147.1, 140.6, 140.2, 129.9, 128.6, 128.3, 126.6, 106.7, 94.2, 83.1, 65.0, 33.8, 31.2. FT-IR (thin film on NaCl, cm^{-1}): 3365, 2963, 2868, 2174, 1652, 1457, 1251, 1028, 698. HRMS (CI) calcd for $C_{28}H_{27}NO_2$ $[M]^+$ 409.2036, found 409.2032.

(2*E*,4*E*,6*E*)-2,4,6-Tris((4-*tert*-butyl-2,6-bis((*S*)-3-hydroxy-3-phenylprop-1-ynyl)phenylamino)methylene)cyclohexane-1,3,5-trione ((*S*,*S*)$_3$-3). A round-bottom flask was charged with **8** (1.05 g, 2.56 mmol), 1,3,5-triformylphloroglucinol (108 mg, 0.514 mmol), and EtOH (20 mL) at room temperature. The reaction mixture was heated at reflux for 30 h, concentrated under reduced pressure, and purified by flash chromatography on SiO_2 (CH_2Cl_2) to furnish (*S*,*S*)$_3$-**3** as a yellow solid (0.70 g, 0.51 mmol, 99%). ^{1}H NMR (400 MHz, $CDCl_3$, 298 K): δ 13.34 (d, J = 13.2 Hz, 3H), 9.43 (d, J = 13.6 Hz, 3H), 7.58−7.50 (m, 18H), 7.24−7.14 (m 18H), 6.13 (d, J = 8.8 Hz, 6H), 5.73 (d, J = 8.4 Hz, 6H), 1.32 (s, 27H); ^{13}C NMR (100 MHz, $CDCl_3$, 298 K): δ 184.8, 151.8, 148.5, 140.5, 138.1, 131.0, 128.3, 128.0, 126.6, 113.6, 106.1, 97.2, 81.9, 64.6, 34.5, 30.9; FT-IR (thin film on NaCl, cm^{-1}): 3370, 2964, 2869, 1603, 1570, 1432, 1302, 1234, 1028, 986, 883. HRMS (ESI) calcd for $C_{93}H_{81}O_9N_3Na$ $[M + Na]^+$ 1406.5865, found 1406.5814.

(1*R*,1′*R*)-3,3′-(2-Amino-5-*tert*-butyl-1,3-phenylene)bis(1-phenylprop-2-yn-1-ol) (9). This compound was prepared with 4-*tert*-butyl-2,6-diiodoaniline (414 mg, 1.03 mmol), (*S*)-1-phenyl-2-propyn-1-ol (300 mg, 2.27 mmol), Et_3N (20 mL), $Pd(PPh_3)_4$ (24 mg, 0.021 mmol), and CuI (6 mg, 0.03 mmol) by a procedure analogous to that used to prepare **8**. This product was isolated as a yellow solid (418 mg, 1.02 mmol, 99%) after flash column chromatography on SiO_2 (hexanes/EtOAc = 1:1). ^{1}H NMR (400 MHz, $CDCl_3$, 298 K): δ 7.64−7.60 (m, 4H), 7.44−7.33 (m, 6H), 7.32 (s, 2H), 5.75 (d, J = 5.6 Hz, 2H), 4.59 (bs, 2H), 2.35 (d, J = 6.0 Hz, 2H), 1.25 (s, 9H); ^{13}C NMR (100 MHz, $CDCl_3$, 298 K): δ 147.1, 140.6, 140.2, 129.9, 128.6, 128.3, 126.6, 106.7, 94.2, 83.1, 65.0, 33.8, 31.2. FT-IR (thin film on NaCl, cm^{-1}): 3366, 2963, 2868, 2174, 1635, 1616, 1457, 1249, 1020, 699. HRMS (CI) calcd for $C_{28}H_{27}NO_2$ $[M]^+$ 409.2036, found 409.2045.

(2*E*,4*E*,6*E*)-2,4,6-Tris((4-*tert*-butyl-2,6-bis((*R*)-3-hydroxy-3-phenylprop-1-ynyl)phenylamino)methylene)cyclohexane-1,3,5-trione ((*R*,*R*)$_3$-3). This compound was prepared with **9** (250 mg, 0.61 mmol), 1,3,5-triformylphloroglucinol (26 mg, 0.12 mmol), and EtOH (10 mL) by a procedure analogous to that used to prepare (*S*,*S*)$_3$-**3**. This product was isolated as a yellow solid (154 mg, 0.111 mmol, 93%) after flash column chromatography on SiO_2 (CH_2Cl_2). ^{1}H NMR (400 MHz, $CDCl_3$, 298 K): δ 13.34 (d, J = 13.2 Hz, 3H), 9.43 (d, J = 13.6 Hz, 3H), 7.58−7.50 (m, 18H), 7.24−7.14 (m, 18H), 6.13 (d, J = 8.8 Hz, 6H), 5.73 (d, J = 8.4 Hz, 6H), 1.32 (s, 27H); ^{13}C NMR (100 MHz, $CDCl_3$, 298 K): δ 184.8, 151.8, 148.5, 140.5, 138.1, 131.0, 128.3, 128.0, 126.6, 113.6, 106.1, 97.2, 81.9, 64.6, 34.5, 30.9. FT-IR (thin film on NaCl, cm^{-1}): 3372, 2963, 1603, 1569, 1432, 1301, 1234, 1028, 985, 883, 697. HRMS (ESI) calcd for $C_{93}H_{81}O_9N_3Na$ $[M + Na]^+$ 1406.5865, found 1406.5890.

(1*S*,1′*S*)-3,3′-(5-*tert*-Butyl-2-((*E*)-2-hydroxybenzylidene-amino)-1,3-phenylene)bis(1-phenylprop-2-yn-1-ol) ((*S*,*S*)-4). This compound was prepared with **8** (50 mg, 0.12 mmol) and salicylaldehyde (5.00 g, 40.9 mmol) by a procedure analogous to that used to prepare (*S*,*S*)$_3$-**3**. This product was isolated as a yellow solid (58 mg, 0.11 mmol, 94%) after flash column chromatography on SiO_2 (hexanes/EtOAc = 20:1 to 4:1, v/v). ^{1}H NMR (400 MHz, $CDCl_3$, 298 K): δ 14.0 (s, 1H), 9.02 (s, 1H), 7.55−7.52 (m, 6H), 7.38−7.26 (m, 7H), 7.00−6.97 (m, 2H), 6.84 (t, J = 7.6 Hz, 1H), 5.67 (d, J = 4.8 Hz, 2H), 3.05 (d, J = 5.2 Hz, 2H), 1.28 (s, 9H); ^{13}C NMR (100 MHz, $CDCl_3$, 298 K): δ 165.7, 161.2, 148.9, 147.6, 140.4, 133.6, 132.5, 130.6, 128.7, 128.4, 126.6, 119.2, 118.9, 117.5, 115.4, 93.8, 83.9, 65.1, 34.5, 31.0. FT-IR (thin film on NaCl, cm^{-1}): 3377, 2963, 2190, 1653, 1457, 1224, 1103, 917, 698. HRMS (CI) calcd for $C_{35}H_{31}O_3N$ $[M]^+$ 513.2298, found 513.2280.

(*S*)-3-(2-Amino-5-*tert*-butyl-3-(3-hydroxyprop-1-ynyl)phenyl)-1-phenylprop-2-yn-1-ol (10). This compound was prepared in iterative two-step Sonogashira−Hagihara cross-coupling reactions. Reaction of 4-*tert*-butyl-2,6-diiodoaniline (1.03 g, 2.57 mmol), (*R*)-1-phenyl-2-propyn-1-ol (310 mg, 2.35 mmol), $Pd(PPh_3)_4$ (60 mg, 0.052 mmol), and CuI (15 mg, 0.079 mmol) in Et_3N (15 mL) with a procedure analogous to that used to prepare **8** furnished (*S*)-3-(2-amino-5-*tert*-butyl-3-iodophenyl)-1-phenylprop-2-yn-1-ol (650 mg, 1.60 mmol, 68%) as a yellow sticky oil after flash column chromatography on SiO_2 (hexanes/EtOAc = 3:1, v/v). ^{1}H NMR (400 MHz, $CDCl_3$, 298 K): δ 7.62 (d, J = 2.4 Hz, 1H), 7.59 (d, J = 7.0 Hz, 2H), 7.43−7.33 (m, 3H), 7.31 (d, J = 2.4 Hz, 1H), 5.73 (bs, 1H), 4.53 (bs, 2H), 3.21 (bs, 1H), 1.25 (s, 9H); ^{13}C NMR (100 MHz, $CDCl_3$, 298 K): δ 145.7, 142.1, 140.6, 136.9, 129.4, 128.7, 128.4, 126.6, 106.4, 94.2, 83.4, 83.3, 65.0, 33.7, 31.2. A portion of this material (330 mg, 0.81 mmol) was carried on to the second coupling step by reacting with propargyl alcohol (458 mg, 8.14 mmol), $Pd(PPh_3)_4$ (19 mg, 0.016 mmol), and CuI (5 mg, 0.03 mmol) in Et_3N (10 mL) by a procedure analogous to that used to prepare **8**. A yellow sticky oil of **10** (160 mg, 0.480 mmol, 59%) was isolated after flash column chromatography on SiO_2 (hexanes/EtOAc = 1:1, v/v). ^{1}H NMR (400 MHz, $CDCl_3$, 298 K): δ 7.60−7.56 (m, 2H), 7.40−7.27 (m, 5H), 5.70 (bs, 1H), 4.73 (bs, 2H), 4.48 (s, 2H), 3.62 (bs, 1H), 3.01 (bs, 1H), 1.22 (s, 9H); ^{13}C NMR (100 MHz, $CDCl_3$, 298 K): δ 147.0, 140.6, 140.3, 130.0, 129.8, 128.7, 128.4, 126.7, 106.9, 106.7, 94.2, 92.6, 83.2, 82.2, 65.0, 51.4, 33.8, 31.2. FT-IR (thin film on NaCl, cm^{-1}): 3363, 2962, 2867, 2172, 1616, 1457, 1252, 1029, 699. HRMS (CI) calcd for $C_{22}H_{23}O_2N$ $[M]^+$ 333.1723, found 333.1722.

(2*E*,4*E*,6*E*)-2,4,6-Tris((4-*tert*-butyl-2-((*S*)-3-hydroxy-3-phenylprop-1-ynyl)-6-(3-hydroxypropynyl)phenylamino)methylene)cyclohexane-1,3,5-trione ((*S*)$_3$-5). This compound was prepared with **10** (150 mg, 0.45 mmol), 1,3,5-triformylphloroglucinol (19 mg, 0.090 mmol), and EtOH (10 mL) by a procedure analogous to that used to prepare (*S*,*S*)$_3$-**3**. This product was isolated as a yellow solid (100 mg, 0.0865 mmol, 96%) after flash column chromatography on SiO_2 (CH_2Cl_2). ^{1}H NMR (400 MHz, $CDCl_3$, 298 K): δ 13.4 (d, J = 13.2 Hz, 3H), 9.64 (d, J = 13.2 Hz, 3H), 7.54 (d, J = 7.2 Hz, 6H), 7.47 (d, J = 6.4 Hz, 6H), 7.24−7.15 (m, 9H), 6.07 (d, J = 7.6 Hz, 3H), 5.72 (d, J = 7.2 Hz, 3H), 5.24 (t, J = 5.6 Hz, 3H), 4.49 (d, J = 4.8 Hz, 6H), 1.27 (s, 27H); ^{13}C NMR (100 MHz, $CDCl_3$, 298 K): δ 185.4, 152.2, 140.3, 138.2, 131.1, 130.9, 128.4, 128.0, 126.6, 113.8, 113.6, 106.3, 97.2, 95.9, 82.0, 81.3, 64.6, 51.1, 34.5, 31.0. FT-IR (thin film on NaCl, cm^{-1}): 3381, 2963, 2867, 2189, 1603, 1570, 1432, 1302, 1235, 1032, 986, 883. HRMS (ESI) calcd for $C_{75}H_{69}O_9N_3Na$ $[M + Na]^+$ 1178.4926, found 1178.4917.

(*S*)-3-(2-Amino-5-*tert*-butylphenyl)-1-phenylprop-2-yn-1-ol (11). This compound was prepared with 4-*tert*-butyl-2-iodoaniline (510 mg, 1.85 mmol), (*R*)-1-phenyl-2-propyn-1-ol (270 mg, 2.04 mmol), Et_3N (10 mL), $Pd(PPh_3)_4$ (43 mg, 0.037 mmol), and CuI (11 mg, 0.058 mmol) by a procedure analogous to that used to prepare **8**. This product was isolated as a yellow solid (510 mg, 1.83 mmol, 99%) after flash column chromatography on SiO_2 (hexanes/EtOAc = 2:1 to 1:1, v/v). ^{1}H NMR (400 MHz, $CDCl_3$, 298 K): δ 7.59 (d, J = 7.2 Hz, 2H), 7.38−7.30 (m, 4H), 7.15 (dd, J = 8.4, 2.0 Hz, 1H), 6.61 (d, J = 8.4 Hz, 1H), 5.70 (s, 1H), 4.09 (bs, 2H), 3.35 (bs, 1H), 1.24 (s, 9H); ^{13}C NMR (100 MHz, $CDCl_3$, 298 K): δ 145.5, 140.9, 140.8, 128.7, 128.6, 128.2, 127.2, 126.6, 114.4, 106.8, 93.9, 83.7, 65.0, 33.8, 31.3. FT-IR (thin film on NaCl, cm^{-1}): 3367, 2961, 2902, 2866, 2172, 1623, 1500, 1263, 1015, 699. HRMS (CI) calcd for $C_{19}H_{21}NO$ $[M]^+$ 279.1618, found 279.1609.

(2*E*,4*E*,6*E*)-2,4,6-Tris((4-*tert*-butyl-2-((*S*)-3-hydroxy-3-phenylprop-1-ynyl)phenylamino)methylene)cyclohexane-1,3,5-trione ((*S*)$_3$-6). This compound was prepared with **11** (500 mg, 1.79 mmol), 1,3,5-triformylphloroglucinol (75 mg, 0.36 mmol), and EtOH (20 mL) by a procedure analogous to that used to prepare (*S*,*S*)$_3$-

3. The product was isolated as a yellow solid (354 mg, 0.356 mmol, 99%) after filtration and washing with EtOH. ^{1}H NMR (400 MHz, $CDCl_3$, 298 K): δ 14.01 (d, J = 13.2 Hz, 3H), 8.78 (d, J = 13.2 Hz, 3H), 7.71 (d, J = 7.2 Hz, 6H), 7.43−7.31 (m, 12 H), 7.25−7.18 (m, 6H), 6.25 (d, J = 5.2 Hz, 3H), 5.84 (d, J = 5.2 Hz, 3H), 1.24 (s, 27H); ^{13}C NMR (100 MHz, $CDCl_3$, 298 K): δ 184.5, 148.1, 147.6, 141.2, 137.8, 128.6, 128.0, 127.8, 127.4, 126.9, 113.6, 113.0, 109.7, 106.6, 81.2, 64.8, 34.5, 31.1. FT-IR (thin film on NaCl, cm^{-1}): 2962, 1617, 1595, 1576, 1451, 1300, 1042, 816. HRMS (ESI) calcd for $C_{66}H_{63}O_6N_3Na$ [M + Na]$^+$ 1016.4609, found 1016.4606.

(*R*)-3-(2-Amino-5-*tert*-butylphenyl)-1-phenylprop-2-yn-1-ol (12). This compound was prepared with 4-*tert*-butyl-2-iodoaniline (284 mg, 1.03 mmol), (*S*)-1-phenyl-2-propyn-1-ol (150 mg, 1.14 mmol), Et_3N (10 mL), $Pd(PPh_3)_4$ (24 mg, 0.021 mmol), and CuI (6 mg, 0.03 mmol) by a procedure analogous to that used to prepare **8**. This product was isolated as a yellow solid (285 mg, 1.02 mmol, 99%) after flash column chromatography on SiO_2 (hexanes/EtOAc = 1:1, v/v). ^{1}H NMR (400 MHz, $CDCl_3$, 298 K): δ 7.59 (d, J = 7.2 Hz, 2H), 7.38−7.30 (m, 4H), 7.15 (dd, J = 8.4, 2.4 Hz, 1H), 6.61 (d, J = 8.4 Hz, 1H), 5.70 (s, 1H), 4.09 (bs, 2H), 3.35 (bs, 1H), 1.24 (s, 9H); ^{13}C NMR (100 MHz, $CDCl_3$, 298 K): δ 145.5, 140.9, 140.8, 128.7, 128.6, 128.2, 127.2, 126.6, 114.4, 106.8, 93.9, 83.7, 65.0, 33.8, 31.3. FT-IR (thin film on NaCl, cm^{-1}): 3362, 3062, 2962, 2903, 2867, 2172, 1635, 1576, 1499, 1264, 1015, 699. HRMS (CI) calcd for $C_{19}H_{21}NO$ [M]$^+$ 279.1618, found 279.1607.

(2*E*,4*E*,6*E*)-2,4,6-Tris((4-*tert*-butyl-2-((*R*)-3-hydroxy-3-phenylprop-1-ynyl)phenylamino)methylene)cyclohexane-1,3,5-trione ((*R*)$_3$-6). This compound was prepared with **12** (280 mg, 1.00 mmol), 1,3,5-triformylphloroglucinol (42 mg, 0.20 mmol), and EtOH (20 mL) by a procedure analogous to that used to prepare (*S,S*)$_3$-**3**. This product was isolated as a yellow solid (170 mg, 0.17 mmol, 86%) after filtration and washing with EtOH. ^{1}H NMR (400 MHz, $CDCl_3$, 298 K): δ 13.92 (d, J = 13.6 Hz, 3H), 8.76 (d, J = 13.6 Hz, 3H), 7.71 (d, J = 7.2 Hz, 6H), 7.43−7.31 (m, 12H), 7.11−7.00 (m, 6H), 6.31 (d, J = 4.8 Hz, 3H), 5.84 (d, J = 4.4 Hz, 3H), 1.21 (s, 27H); ^{13}C NMR (100 MHz, $CDCl_3$, 298 K): δ 184.5, 148.1, 147.6, 141.2, 137.8, 128.6, 128.0, 127.8, 127.4, 126.9, 113.6, 113.0, 109.7, 106.6, 81.2, 64.8, 34.4, 31.1. FT-IR (thin film on NaCl, cm^{-1}): 2952, 2187, 1616, 1595, 1448, 1345, 1299, 815. HRMS (ESI) calcd for $C_{66}H_{63}O_6N_3Na$ [M + Na]$^+$ 1016.4609, found 1016.4606.

(2*E*,4*E*,6*E*)-2,4,6-Tris((4-*tert*-butyl-2-((*S*)-3-phenyl-3-(trimethylsilyloxy)prop-1-ynyl)phenylamino)methylene)cyclohexane-1,3,5-trione ((*S*)$_3$-7). To a THF solution (5 mL) of (*S*)$_3$-**6** (21.1 mg, 0.021 mmol) and Et_3N (0.20 mL, 1.4 mmol) under N_2 atmosphere was added TMSCl (0.20 mL, 1.6 mmol). The reaction mixture was stirred at rt for 48 h. Volatile fractions were removed under reduced pressure and the yellow residual material was extracted into hexanes, filtered through glass wool, and concentrated under reduced pressure to afford (*S*)$_3$-**7** as a yellow solid (25.7 mg, 100%). ^{1}H NMR (400 MHz, $CDCl_3$, 298 K): δ 13.69 (d, J = 13.0 Hz, 3H), 8.76 (d, J = 13.6 Hz, 3H), 7.77 (d, J = 7.6 Hz, 6H), 7.49 (d, J = 2.0 Hz, 3H), 7.42−7.26 (m, 15H), 6.15 (s, 3H), 1.31 (s, 27H), 0.30 (s, 27H); ^{13}C NMR (100 MHz, $CDCl_3$, 298 K): δ 185.1, 147.8, 141.4, 138.7, 129.7, 128.4, 127.8, 127.1, 126.6, 114.0, 113.2, 107.6, 97.3, 81.0, 65.2, 34.5, 31.2, 0.3. FT-IR (thin film on NaCl, cm^{-1}): 2961, 2903, 2869, 1613, 1587, 1445, 1344, 1289, 1266, 1251, 1230, 1088, 1064, 996, 874, 844, 752, 697. HRMS (ESI) calc for $C_{75}H_{88}N_3O_6Si_3$ [M + H]$^+$ 1210.5981, found 1210.5944.

Density Functional Theory Calculations. All calculations were performed using density functional theory (DFT). Initial structures were constructed in Cerius[60] and constrained with C_3-symmetry with Maestro.[61] Geometry optimizations were performed using Jaguar 6.0 suite[62] of ab initio quantum chemistry program employing the B3LYP/6-31G** level of theory.[63,64] The energies of the optimized structures were reevaluated by additional single-point calculations on each optimized geometry using Dunning's correlation-consistent triple-ζ basis set cc-pVTZ(-f).[65] Solvation energies were calculated using a self-consistent reaction field (SCRF) method and conductor-like screening model (COSMO) was employed.[66,67] Empirical parameters such as dielectric constant (ε = 4.806, $CHCl_3$) and atomic radii (H, 1.140 Å; C, 1.900 Å; O, 1.600 Å) were used to construct the solute surface.

The free energy in solution phase, G_{sol}, was calculated by following standard protocol:

$$G_{sol} = G_{gas} + G_{solv} \quad (2)$$

$$G_{gas} = H_{gas} - TS_{gas} \quad (3)$$

$$H_{gas} = E_{SCF} + ZPE \quad (4)$$

where G_{gas} = free energy in gas phase; G_{solv} = free energy of solvation as computed by using the continuum solvation model; H_{gas} = enthalpy in gas phase; T = temperature (= 298.15 K); S_{gas} = entropy in the gas phase; E_{SCF} = self-consistent field energy, i.e. "raw" electronic energy as computed from the SCF procedure; ZPE = zero point energy. Considering the energy difference of ~12 kcal mol^{-1} computed for (*M*)-(*S,S*)$_3$-**2** and (*P*)-(*S,S*)$_3$-**2** (Table S1 [SI]), the contribution of TS_{gas} and ZPE terms are negligibly small and thus approximated to be zero.

In order to simulate the UV−vis and CD spectra, time-dependent density functional theory (TD-DFT) was employed. The calculation of individual excitation was carried out with the Amsterdam Density Functional (ADF) software package[68] using the generalized gradient approximation (GGA) functional BP86/LB94 and the triple-ζ polarized (TZP) standard ADF basis set on all atoms.[64,69]

The intensity of each electronic transition in calculated UV−vis spectrum is represented by the oscillator strength, f, given in eq 5,[70] where ε is the molar absorptivity and $\bar{\nu}$ is the frequency in wavenumbers.

$$f = 4.315 \times 10^{-9} \int \varepsilon \bar{\nu} \quad (5)$$

For the calculation of CD spectrum, rotatory strength, R, was obtained by eq 6,[71,72] where $\Delta\varepsilon$ (in M^{-1} cm^{-1}) is the difference in the molar absorptivity for the left- and right-handed circular polarized light and $\bar{\nu}^o$ is the center of the band.

$$R = 22.94 \int \frac{\Delta\varepsilon(\bar{\nu})}{\bar{\nu}} d\bar{\nu} \approx \frac{22.94}{\bar{\nu}^o} \int \Delta\varepsilon(\bar{\nu}) d\bar{\nu} \quad (6)$$

Rotatory strengths in the calculated ECD spectra were reported in the velocity representation of the electric transition dipole moment and in centimeter·gram·second (c.g.s) units of 10^{-40} esu cm erg/G.[71−73] Gaussian line shapes were assumed for individual

(60) *Cerius2*, v 4.8.1; Accelrys Inc.: San Diego, CA, 2003.
(61) *Maestro*, v 6.5.007; Schrödinger Inc.: Portland, OR, 2004.
(62) *Jaguar*, v 6.0; Schrödinger, Inc.: Portland, OR, 2003.
(63) Becke, A. D. *J. Chem. Phys.* **1993**, *98*, 5648–5652.
(64) Becke, A. D. *Phys. Rev. A* **1988**, *38*, 3098–3100.
(65) Dunning, T. H., Jr *J. Chem. Phys.* **1989**, *90*, 1007–1023.
(66) Klamt, A.; Schürmann, G. *J. Chem. Soc., Perkin Trans. 2* **1993**, 799–805.
(67) Pye, C. C.; Ziegler, T. *Theor. Chem. Acc.* **1999**, 396–408.
(68) te Velde, G.; Bickelhaupt, F. M.; Baerends, E. J.; Guerra, C. F.; van Gisbergen, S. J. A.; Snijders, J. G.; Ziegler, T. *J. Comput. Chem.* **2001**, *22*, 931–967.
(69) Perdew, J. P. *Phys. Rev. B* **1986**, *33*, 8822–8824.
(70) Drago, R. S. *Physical Methods for Chemists*, 2nd ed.; Surfside Scientific Publishers: Gainesville, FL, 1992.
(71) Autschbach, J.; Ziegler, T.; van Gisbergen, S. J. A.; Baerends, E. J. *J. Chem. Phys.* **2002**, *116*, 6930–6940.
(72) Dierksen, M.; Grimme, S. *J. Chem. Phys.* **2006**, *124*, 174301-1–174301-12.
(73) Pulm, F.; Schramm, J.; Hormes, J.; Grimme, S.; Peyerimhoff, S. D. *Chem. Phys.* **1997**, *224*, 143–155.

electronic excitations in the calculated CD spectra,[74] which were scaled by empirically adjusting the linewidths for a qualitative comparison with the experimentally obtained spectrum.

Acknowledgment. This work was supported by the National Science Foundation (CAREER CHE 0547251), the U.S. Army Research Office (W911NF-07-1-0533), and the Alfred P. Sloan Foundation. We thank Xiaofan Yang and Richard Lord of the Baik group at Indiana University for helpful discussions on DFT studies. This paper is dedicated to Professor Junghun Suh on the occasion of his 60th birthday.

Supporting Information Available: Additional spectroscopic data and DFT calculations. This material is available free of charge via the Internet at http://pubs.acs.org.

JA806723E

(74) Harada, N.; Nakanishi, K. *Circular Dichroic Spectroscopy: Exciton Coupling in Organic Stereochemistry*; University Science Books: Mill Valley, CA, 1983.